Non-Contact Neonatal Heart Rate Monitoring Using Blue Filter Technique with Photoplethysmography Imaging under UV Illumination

Huda Ali Hashim
Middle Technical University, Electrical Engineering Technical College, Baghdad, Iraq
e-mail: huda.ali@mtu.edu.iq

Abstract. Non-contact heart rate (HR) monitoring is essential for neonates, as traditional adhesive sensors can damage their delicate skin. The rise in contagious viral infections further emphasizes the need for contactless neonatal healthcare monitoring systems to reduce physical interaction and the risk of disease transmission. This study proposes a novel non-contact HR monitoring system for neonates, combining a blue-filter technique with skin color enhancement under UV illumination. The system utilizes digital camera-based photoplethysmography imaging and a tile-based region of interest (ROI) selection method. Also, a neonatal graphical user interface (GUI) was developed for real-time HR monitoring and clear visualization of findings. We compared the findings of the proposed technique with standard UV photoplethysmography imaging without the blue filter technique to validate its effectiveness. Experimental findings demonstrate the proposed system's high performance, with a Pearson correlation coefficient (PCC) of 0.998 and a mean absolute error (MAE) of 1.12 bpm, closely matched to ECG monitor readings. These findings highlight the system's potential as a reliable, non-contact solution for neonatal HR monitoring in the NICU, offering a promising advancement in neonatal care and broader biomedical applications.

Keywords: heart rate; neonatal; digital camera; biomedical.

Paper #9219 received 14 Jan 2025; revised manuscript received 8 Feb 2025; accepted for publication 13 Mar 2025; published online 29 Mar 2025. doi: 10.18287/JBPE25.11.010305.

1 Introduction

Monitoring neonatal heart rate is critical for accurately and continuously assessing their health status [1, 2]. This process facilitates the early detection of changes in temperature, heart rate, or respiratory patterns, enabling timely interventions to enhance safety and mitigate potential health risks [3, 4]. In emergency situations, traditional heart rate monitoring devices primarily rely on contact-based sensors, such as electrodes, probes, or straps [5]. These methods often involve adhesive biosensors and electrodes [6], such as those utilized for electrocardiograms (ECG), spirometry, and pulse oximetry [7]. However, the application and removal of these sensors can damage the delicate skin of neonates and restrict their mobility, posing additional challenges in clinical settings [8].

In contrast, non-contact approaches to vital sign monitoring have emerged as a crucial area of research in biomedical and clinical applications [3, 4, 9]. These methods aim to minimize physical interaction and reduce the risk of disease transmission, particularly in the context of highly contagious environments. Such advancements hold significant promise for improving neonatal care while addressing the limitations of traditional contact-based systems [10].

Nevertheless, noise and motion artifacts mostly influence the previous non-contact approaches; these techniques are vulnerable to noise and motion artifacts, which restrict mobility [11]. Moreover, they pose risks to human health and may have various biological effects on physiological tissues [12, 13]. Moreover, they possess a limited distance range and need a region area of interest (ROI) for analytical measurements [14]. Consequently, limiting the patient's distant mobility poses a significant challenge owing to the expense of the sensor, which hinders the collection of sufficient bodily samples. Their poor resolution limits the detection range. Moreover, the emitted radar radiation is likely detrimental to human health and may induce various biological consequences on bodily tissues in the future [15, 16].

These imperceptible cardiac signals may be very beneficial, particularly in biological and therapeutic contexts. Blood circulation induces small variations in human skin color that may be amplified to evaluate and extract important information on cardiac activity when epidermal tissue is lit, since hemoglobin absorbs light more effectively than the adjacent epidermal tissue [17, 18]. Consequently, many studies have enhanced a computer vision approach using video cameras as non-contact sensors [19].

Vital signs may be extracted from certain regions of the human epidermis using video camera imaging, which is an appropriate non-contact method. This innovative approach may be classified into 2 primary categories: color-based method, often known as imaging photoplethysmography (PPG) [20] and motion-based method [9]. Several studies [21−23] used color-based methods for non-contact monitoring of cardio signals. However, they obtained PPG signals at small distances of 0.07–0.25 m [24, 25], 0.5 m [26], 0.35 m [27], and 1–1.5 m [28]. Gibsonet et al. [29] introduced a non-contact infant HR value monitoring method. The proposed method uses 2 Nikon cameras to detect face color variations resulting from blood perfusion. The ROI was manually designated by delineating a box around the face. Poh et al. [30] presented a PPG-based video technique that used RGB data from the face area to measure HR values. The ROI was manually delineated in the early frames, whereas later frames used optical flow tracking. However, the proposed technique of optical flow tracking encountered considerable motion artifacts, resulting in inaccuracies in heart rate estimates. Alnaggar et al. [31] proposed new non-contact techniques for RR and HR estimation from the subjects' faces. The recorded videos are magnified using the magnification technique and then analyzed. The HR estimate was achieved by employing face mesh to annotate the boundaries by additional annotating for the boundaries of the most ROI from the face image in both HSV and RGB and color images.

According to a review of the literature, the manual ROI selection method was mostly used for non-contact biological signal monitoring and had issues, such as the fact that adding the bounding boxes by hand was time-consuming and prone to error, which made the extracted HR signals less consistent and reliable. The previous methods were also inadequate in managing subject or patient motion, which might result in the face moving beyond the designated ROI. Moreover, the findings illustrate the constraints of the remote sensing technique in terms of range and field of vision. It has a restricted operational range of less than 1.5 m from the body. Furthermore, the existing studies reveal a substantial and important gap owing to the inadequate investigation of non-contact neonatal vital sign monitoring in the NICU under UV illumination. The aforementioned limitations serve as the impetus for developing a monitoring system for neonatal HR values under UV illumination.

The primary goal of this study is to implement a neonatal healthcare system for non-contact monitoring. This work investigates the effectiveness of a proposed blue filter technique combined with a proposed neonatal ROI selection method to accurately extract HR values under UV illumination in the NICU settings. The contributions of this work are as follows:

- A non-contact neonatal HR monitoring system utilizing digital camera technology under UV illumination was developed.
- A new integration of the blue filter technique and EVM method was proposed to enhance neonatal cardiac signal extraction under UV illumination by reducing noise and amplifying subtle skin color variations.
- A robust tile-based ROI selection method for neonatal cardiac signal monitoring was introduced, ensuring accurate heart rate calculation despite infant movements, and eliminating the need for manual bounding box adjustments.
- A neonatal Graphical User Interface (GUI) system was designed and implemented to facilitate real-time monitoring and visualization of outcomes from the proposed non-contact heart rate monitoring system.

2 Methods and Materials

2.1 Subjects

We conducted this work at the Child Central Teaching Hospital (CCTH) in Baghdad, Iraq. We obtained consent from guardians to image videos using non-contact technology at suitable times when neonates are in quiet positions. We implemented this work after explaining its nature and the experiment's aim to collect samples without any contact with babies. We kept the neonate's identities by covering their faces. In this study, we utilized an ECG device monitor as a reference to evaluate and compare the performance of the 2 suggested experiments for evaluating the HR of neonates.

2.2 Experiment Setup

In this study, we implemented 2 experiments to evaluate a noncontact technique for calculating neonates' heart rates. We conducted both experiments under UV illumination. The first experiment investigates the ability of the proposed noncontact technique to calculate neonatal heart rates using a blue filtering approach applied to phototherapy imaging; thus, it will be referred to as the HRBF experiment, while the second experiment calculates neonate heart rates without employing the blue filtering technique under UV illumination, termed the HRWB experiment.

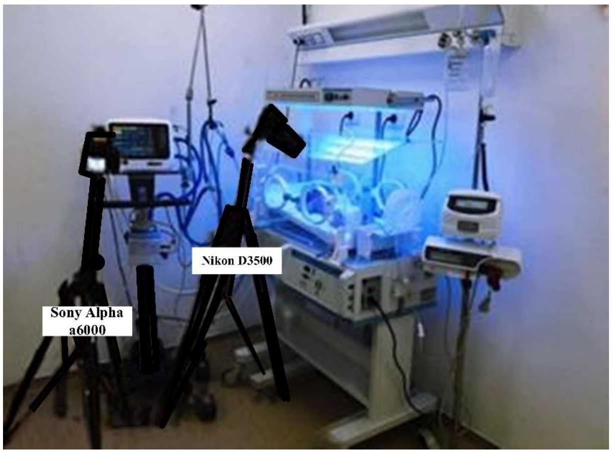

Fig. 1 Experimental setup of neonate's recorded.

We divided 10 neonates into 2 groups: 5 neonates participated in the HRBF experiment, while the remaining 5 were involved in the HRWB experiment. The neonates' gestational ages ranged from 25 to 39 weeks, and their weights varied between 1450 and 3300 g. Fig. 1 depicts the experimental setup, utilizing 2 digital cameras to record video clips. A Nikon D3500 camera, capable of recording at a resolution of 1920 × 1080 px at 30 fps (frames per second), was tripod-mounted at a distance of 0.55–1.5 m to capture videos of the neonates. A Sony Alpha a6000 camera, also tripod-mounted, recorded vital signals displayed on the ECG monitor.

We synchronized both cameras to start recording simultaneously, ensuring consistent timing between the ECG data and the contactless measurements. We stored all videos in MOV format. Data collection in a neonatal intensive care unit (NICU) is inherently challenging due to the delicate environment and the need for minimal interference with medical devices. To validate our study, we created a small database by recording neonates when they were stationary and under continuous ECG monitoring. We maintained the camera-to-subject distance at 1.5–2.5 m. We recorded 20-s clips for each neonate, capturing five clips per neonate for analysis and comparison. In total, we collected 50 clips for each experimental condition (HRBF and HRWB), resulting in a robust dataset for evaluating the proposed technique.

3 System Framework

This section will present the developed healthcare system proposed based on a non-contact HR values monitoring system for neonates. It will include details on the blue filter technique proposed, a tile-based ROI selection technique, a neonatal heart rate calculation technique, and a neonatal graphical interface system proposed. Fig. 2 illustrates the framework of the proposed non-contact neonatal HR monitoring.

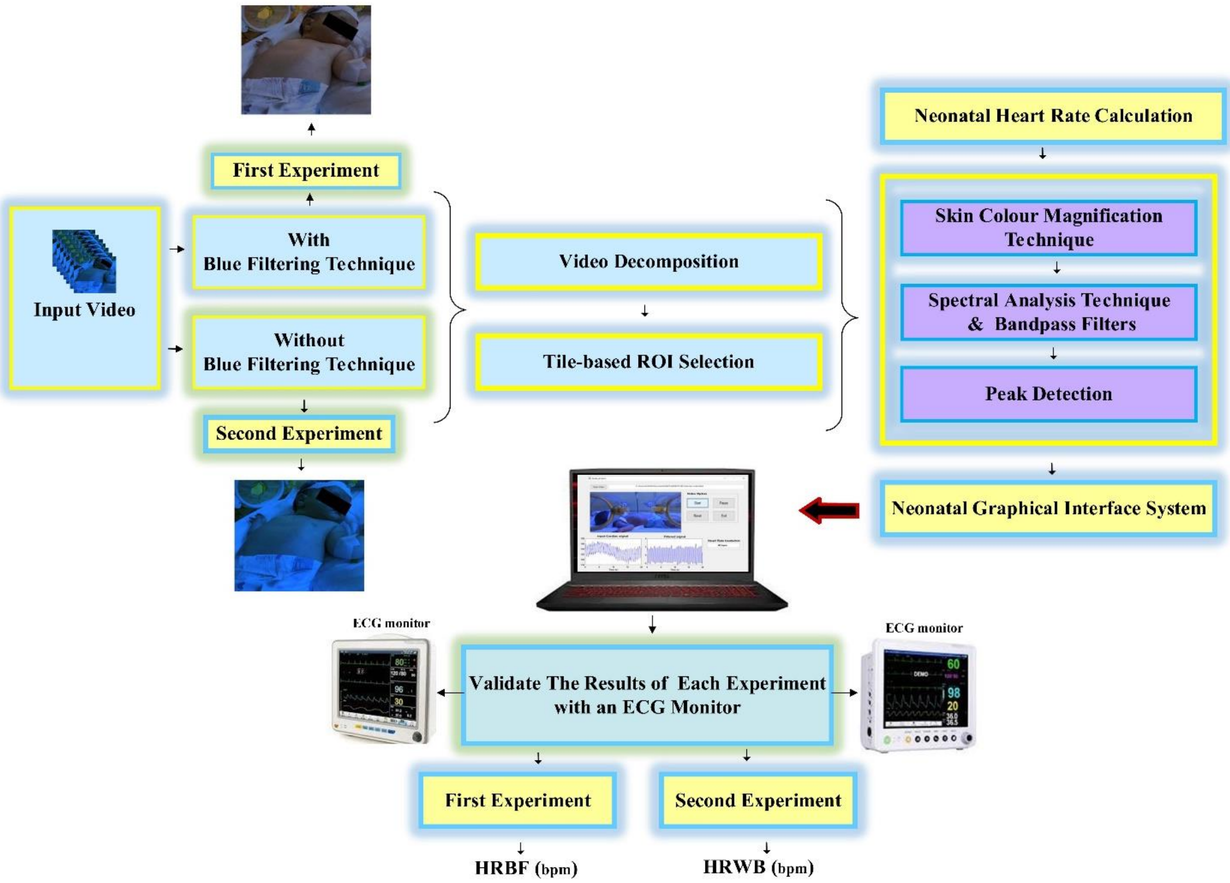

Fig. 2 The system framework of the proposed study.

3.1 Blue Filtering Technique

The basic principle that relies on the PPG is that blood absorbs light more effectively than adjacent tissues. This absorption induces slight alterations in skin pigmentation as a result of cardiovascular activity. The reflectance characteristics of human skin, obtained from video recordings using PPG, provide significant insights into cardiovascular health, including heart rate and blood oxygen saturation [32]. In PPG-based analysis, cyclical alterations in face skin color are shown as changes in brightness (intensity) values within picture sequences, facilitating the detection of heartbeats.

The second principle addresses the challenge of phototherapy images captured under UV light, where the blue channel is dominant compared to the red and green channels. In contrast, natural photographs exhibit a more balanced distribution among the 3 color channels (RGB). To address this disparity, we propose a blue filter technique using the color space transforming method for phototherapy photos in the HRBF experiment. This technique equalizes the image by calibrating the intensity of the red (Adj_R)and blue (Adj_B) channels to align with the brightness of the green channel.

We compute the adjustments for the red and blue channels using the following Eqs.:

$$Adj_R = \frac{1}{w \times h}\left[\sum_{i=1}^{w}\sum_{i=1}^{h} G_{ij} - \sum_{i=1}^{w}\sum_{i=1}^{h} R_{ij}\right], \quad (1)$$

$$Adj_B = \frac{1}{w \times h}\left[\sum_{i=1}^{w}\sum_{i=1}^{h} B_{ij} - \sum_{i=1}^{w}\sum_{i=1}^{h} G_{ij}\right]. \quad (2)$$

Next, we calculate the updated pixel intensities for the red (R_{ij}) and blue (B_{ij}) channels by applying the following Eqs.:

$$R_{ij} = min(255, R_{ij} + Adj_R), \quad (3)$$

$$B_{ij} = max(0, B_{ij} + Adj_B). \quad (4)$$

The introduced blue-filtering technique will enhance the performance and reliability of heart rate measurements during UV phototherapy by reducing inter-channel discrepancies to be similar relatively to obtained images framed from natural illumination.

3.2 Video Decomposition

The raw video is initially decomposed into tiles on the first frame, with each frame being divided into smaller segments corresponding to a grid. The tile size, denoted as $D \times D$, is selected based on heuristic methods. Tile creation begins at the (1,1) coordinate of the raw image frame. In cases where the image width (w) or height (h) is not an exact multiple of D, the tiles do not fully cover the entire raw image frame. Each grid cell represents a distinct tile video. This tile-based division is consistent across all frames in the video, so each frame is divided into a similar yellow grid structure for 2 proposed experiments (HRBF and HRWB), as shown in Fig. 3(a) and (b). The total number of tiles is calculated as follows:

$$T_n = (w/D \times h/D), \quad (5)$$

where, w and h refer to the width and height of the raw image frame, respectively. For each ROI, the tile video is constructed to match the raw video in terms of the number of frames and frame rate.

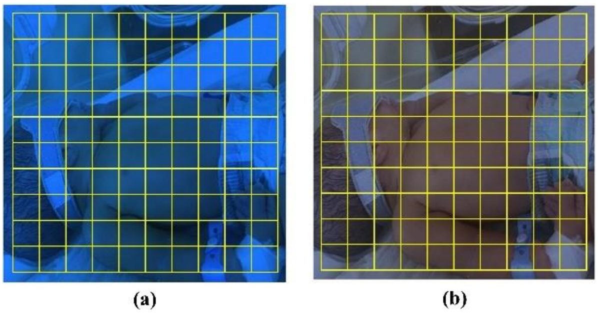

Fig. 3 Image decomposed into tiles: (a) HRBF, (b) HRWF.

3.3 Tile-Based ROI Selection

In this study, we employed a tile-based ROI selection approach for extract cardiac signals from PPG. Each ROI was extracted from the decomposed UV photograph, with the tile grid encompassing the neonatal chest region, which was designated as the ROI for heart rate calculation in two proposed. This procedure was repeated across all frames.

Traditionally, manual ROI selection techniques delineate the chest or head region by enclosing it within a bounding box, from which vital indicators are retrieved. In contrast, our proposed technique selects the tiles containing the region of interest through visual inspection rather than relying on manual bounding boxes.

The primary advantage of this tile-based ROI selection for neonates is that it eliminates the need for constant adjustments when the infant changes posture. As the neonate typically moves laterally, the chest region remains consistently within the initially designated tiles. The adjustable tile size enables us to establish a safe dimension that accommodates the neonate's dynamic movements.

3.4 Neonatal Heart Rate Calculation

This study used a color-based technique to extract the cardiac signal as the first step, utilizing the principle of light absorption by hemoglobin in blood. Hemoglobin absorbs more light than the surrounding tissue, resulting in subtle color variations in the infant's skin that are invisible to the naked eye but detectable with a digital camera. The changes in blood volume within the microvascular tissue during each cardiac cycle reflected in these color variations serve as a means to measure the heart rate. To measure the cardiac signal, the green channel of the RGB color space was selected, as it provides the strongest cardiac frequency signal due to higher absorption in this wavelength. The spatial averaging from the brightness of the pixels within the ROI was then calculated to extract the raw cardiac signal, as described by Eq. (6). This step minimizes the influence of camera noise associated with individual pixels, thereby improving the signal-to-noise ratio. The resulting process effectively reduces noise and enhances the clarity of the cardiac signal representation.

$$I_{G\ (t)} = \frac{\sum_{x,y\in\ ROI} I(x_i,y_i,t)}{|\ ROI|}, \quad (5)$$

where $I\ (x_i,y_i,t)$ is indicated as the illuminance values at the pixel image position (x_i,y_i) at time phase (t), and $|ROI|$ specifies the size of the recorded video selected by *ROI*. The neonatal cardio signal obtained from the *G* channel information was selected for calculate the neonatal HR values of 2 experiments (HRBF and HRWB).

In the second step, we applied a magnification technique to further improve the cardiac signal's extraction and clarity. Based on the EVM technique [31], this technique of magnification brings out small changes in color over time that are caused by the heart's pulsed blood flow. We then add this enhanced signal back to the original video frame to create a clearer representation of the heart rate-related changes in skin color. This magnification approach enhances the cardiac signal extraction and amplification, enabling improved detection of tiny fluctuations, especially when the baby is far from the camera or in low signal-to-noise ratio conditions. This enhanced methodology considerably elevates the dependability and sensitivity of non-contact heart rate monitoring devices.

In the third step, the raw time series cardio signals were converted from the time domain to the frequency domain using the spectrum analysis method using FFT. Subsequently, to get the desired frequency band, 2 ideal band-pass filters were used at 1 Hz to 3 Hz [33], equivalent to the neonatal pulse range of 60 to 180 bpm. Following this, the inverse FFT was applied to the filtering signals to derive the time series of the neonatal cardiac signals.

In the fourth step, temporal sequence neonatal cardiac signals are analyzed by determining the peaks and their respective positions (*locs*) between consecutive peaks. The MATLAB function "findpeaks" was used to identify peaks. The total cycle length between 2 peaks is determined using the following Eq. (7):

$$T_C = mean\left(diff\ (locs)\right). \quad (7)$$

The number of peaks pk can be calculated by the following Eq. (8):

$$pk = \frac{T}{T_C}, \quad (8)$$

where *T* is the duration time in seconds of the recording video.

Finally, the measured values *HR* in bpm (beats per minute) is calculated using Eq. (9):

$$HR = \frac{60\ Pk}{\mathrm{T}}. \quad (9)$$

3.5 Neonatal Graphical Interface System

We implemented a neonatal GUI system for non-contact HR values monitoring using MATLAB 2023b. The proposed system features a user-friendly interface that includes neonatal cardio signal processing and displays the neonatal HR value findings based on integrating a blue-filter technique with skin color magnification under UV illumination. It also offers an efficacious environment for neonatal video uploads.

The proposed system includes text fields for displaying HR values. Additionally, it includes a variety of uploaded neonatal video controls, such as start, pause, extract, and reset options. Moreover, it includes analytical tools, including 3 axes for neonatal video upload, input cardio signal display, and filtered signal output.

4 Experimental Results

4.1 Blue Filter and ROI Selection Proposed

This section presents the performance of the blue filter technique and tile-based ROI selection of 2 experiments. Fig. 4 compares the original image with phototherapy images, both before and after applying the blue filtering method. Fig. 4 shows that the proposed blue-filtering method works to improve the accuracy and reliability of HR measurements during UV phototherapy by reducing differences between channels and reducing the blue tint significantly, especially in areas of skin that can be seen. Other areas, such as neonatal eye masks, bedding, and the incubator bed, also exhibit reduced blue hues, simulating conditions of natural light illumination. This approach plays a crucial role in achieving consistent and clinically meaningful outcomes in neonatal NICU settings under UV illumination.

Fig. 5(a) and (b) show the tile-based ROI selection method utilized in the HRWB and HRBF experiments. As demonstrated in Fig. 5(a) yellow tile encapsulates the neonatal chest region, which was identified as the ROI for heart rate (HR) evaluation. This ensures accurate heart rate calculation despite infant movements and eliminates the need for manual bounding box adjustments This targeted selection ensures the accurate extraction of HR values by focusing on a relevant anatomical area, minimizing interference from non-relevant regions.

4.2 Heart Rate Extraction

In our works, we obtained raw cardio signals for 600 frames by applying spatial averaging to detected

ROIs using a color -based technique. Fig. 6(a) and (b) illustrates the cardio signal from the HRWB and HRB experiments, respectively.

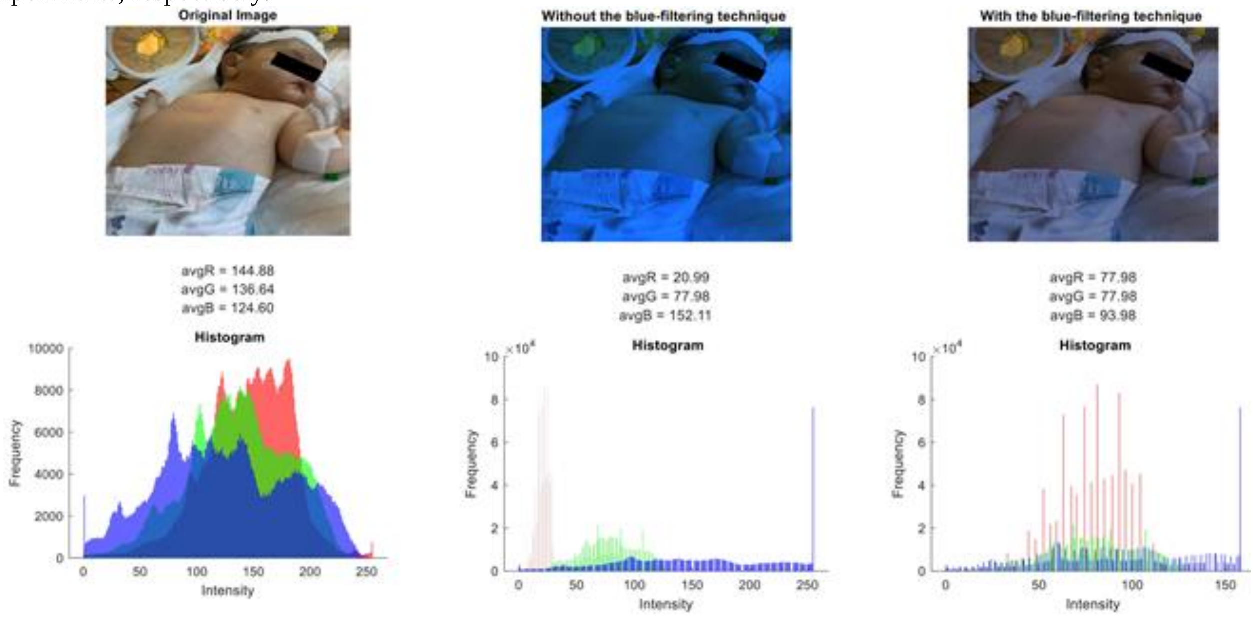

Fig. 4 Comparison of phototherapy images captured with and without the blue-filtering technique.

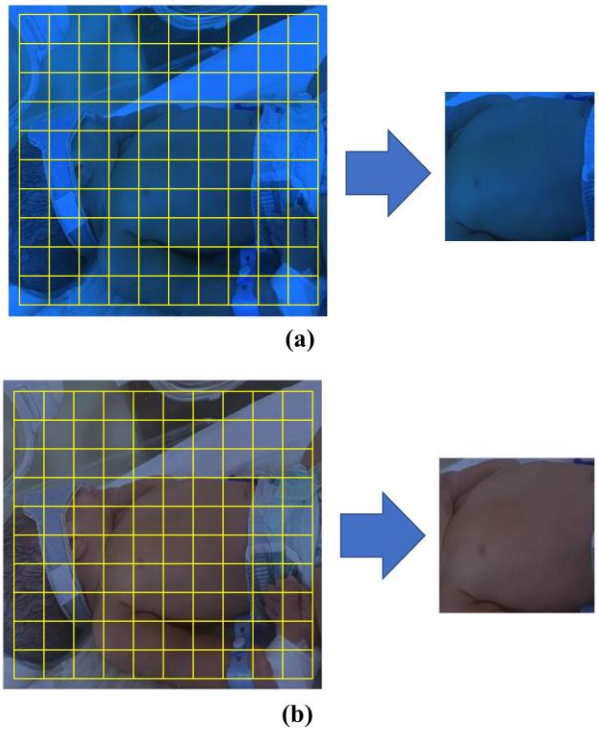

Fig. 5 Tile-based ROI selection of two experiments. (a) HRWB experiment; (b) HRBF experiment.

Fig. 7(a) and (b) displays the cardio signal extraction after applying the magnification technique for two experiments, respectively. the magnification technique extracted the cardiac signal more accurately and amplified it, enabling better detection of subtle variations. This magnified approach significantly improves the reliability and sensitivity of non-contact heart rate monitoring systems.

Fig. 8 (a) and (b) demonstrations the results of filtered with detection peaks cardio signals obtained after applying FFT, band-pass filtering, inverse FFT, and Eq. (7), respectively. In this work, the window duration of FFT was twenty seconds. The green color points indicate the peak positions of the filtered signals, as displayed in Fig. 8(a) (HRWB experiment) and Fig. 8(b) (HRBF experiment).

Fig. 9 shows the neonate's GUI monitoring proposed, which contains the HR values (bpm) calculation after applying Eq. (8), the cardio input signal, and the filtered cardio signal. Additionally, this suggested healthcare system enables real-time remote monitoring of neonates' states and automatically stores cardio signals and HR measurement outputs on the computer as accessible medical data to assist in future diagnoses of neonatal cardio disease.

4.3 Statistical Analysis

This section compares the performance of two experiments (HRWB and HRBF) by analyzing the measured values (HR) by Eq. (9) and reference readings (ECG) using statistical analysis to validate the proposed technique. The statistical analysis methods will be applied, including linear regression, Pearson's correlation coefficient (PCC), Bland-Altman plots, mean bias, Spearman's correlation coefficient (SCC).

The total sample size collected from neonatal captured video was set at n = 25. The statistical analyses of the samples measured readings collected from the HRWB experiment, as shown in Fig. 10a. The Bland-Altman analysis discloses a mean bias of −2.9 bpm, with 95% limits of agreement ranging from −11 to +5. Also, the PCC and SCC results between the measured and reference readings were 0.981 and 0.948, respectively. Fig. 10(b) displays the linear regression analysis of the relationship between the experimental measure readings and the linear fit obtained, with an R^2 value of 0.963.

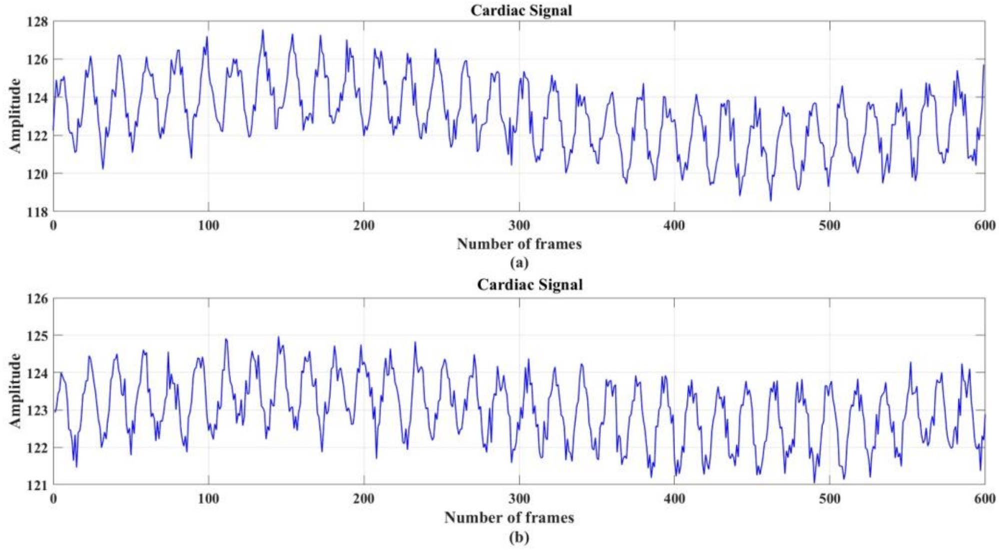

Fig. 6 Raw cardio signals of two experiments. (a) HRWB experiment, (b) HRBF experiment.

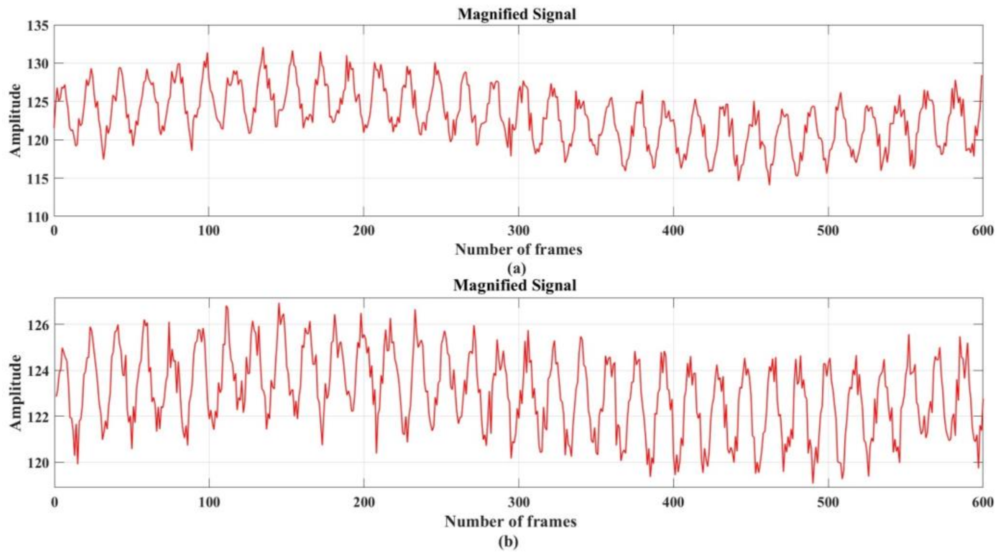

Fig. 7 Magnification results of the raw cardio signals. (a) HRWB experiment, (b) HRBF experiment.

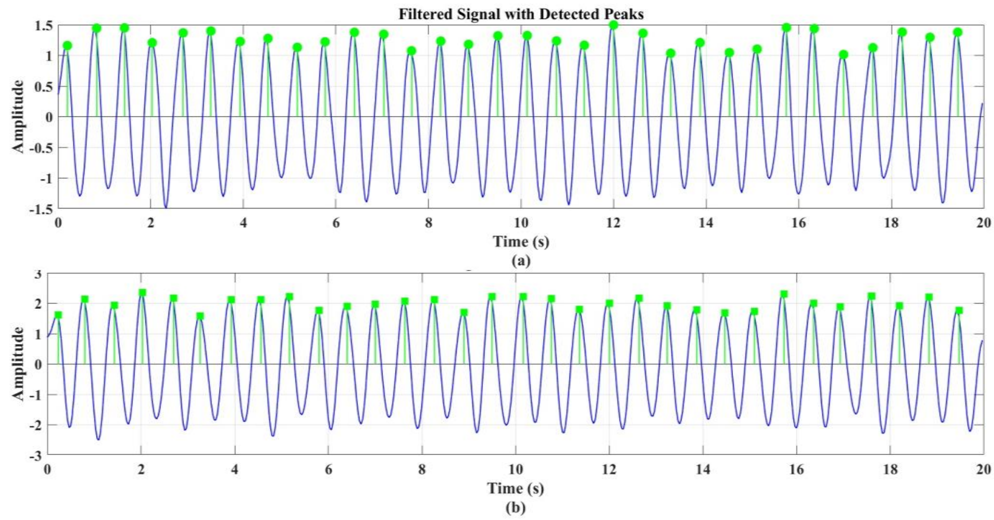

Fig. 8 Filtered and detection peak of cardio signals. (a) HRWB experiment, (b) HRBF experiment.

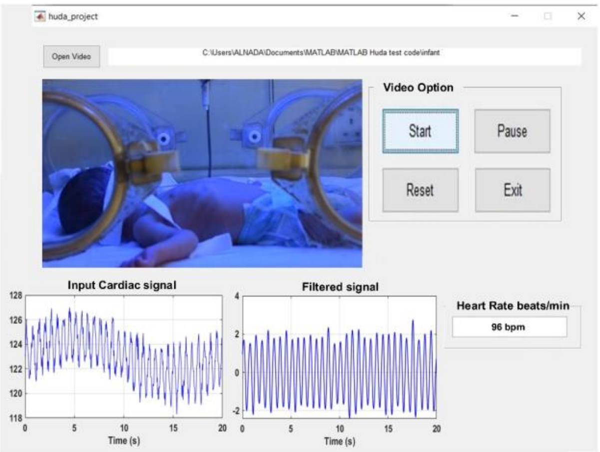

Fig. 9 Screenshot of proposed neonatal system GUI.

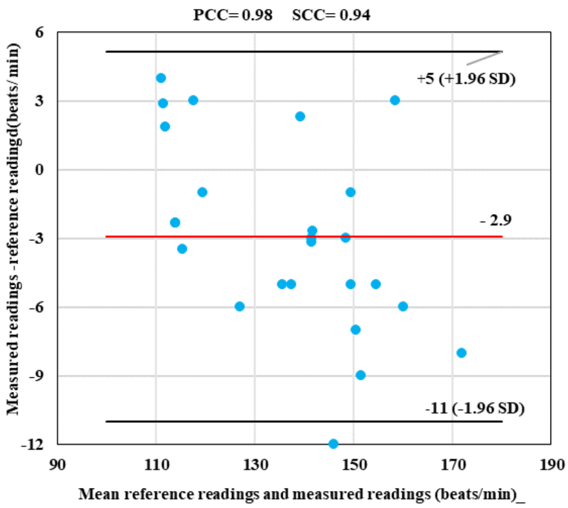

(a)

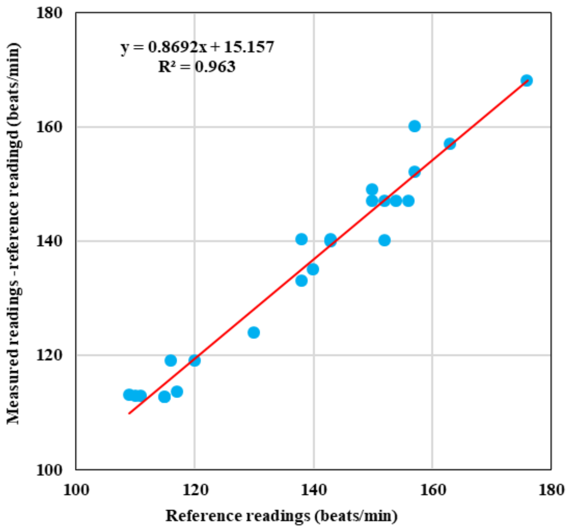

(b)

Fig. 10 Statistical analyses of the HRWB experiment: (a) Bland-Altman plot, (b) correlation plot.

Fig. 11 shows a statistical approach related to measured readings from the HRBF experiment. As demonstrated in Fig. 11(a), the Bland-Altman statistics display a mean bias of 0.39 bpm, with 95% confidence intervals ranging from −1.81 to +2.59. Also, the highest obtained results of the PCC and SCC between readings and reference readings were 0.998 and 0.982, respectively. Also, the linear regression coefficients demonstrate a strong match output between the values of measured readings and the linear fit, with R^2 = 0.995, as shown in in Fig. 11(b).

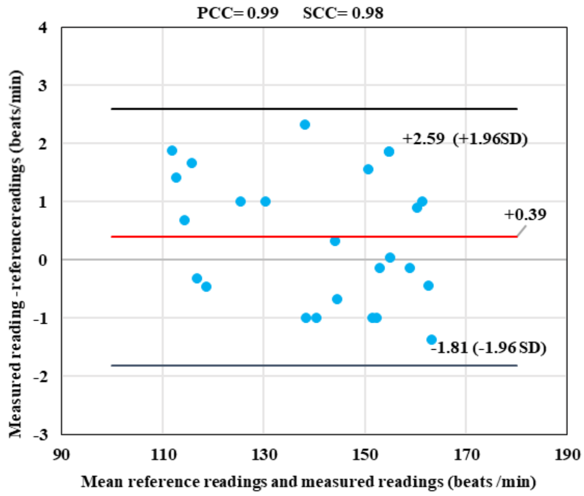

(a)

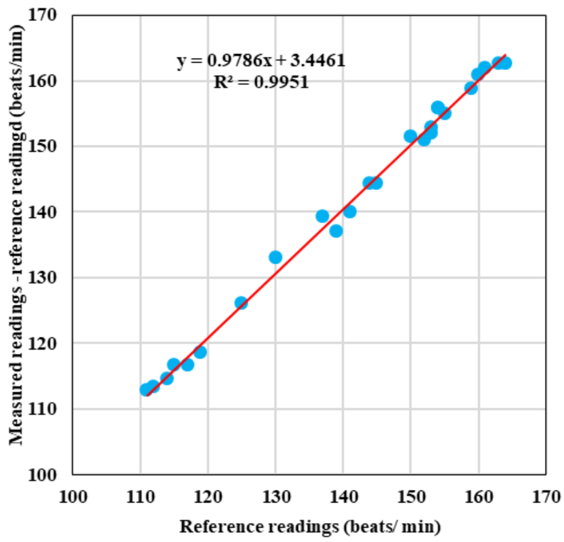

(b)

Fig. 11 Statistical analyses of the HRBF experiment: (a) Bland-Altman plot, (b) correlation plot.

To validate the proposed technique, the performance results from the HRBF experiment were compared with those from the HRWB experiment. The findings demonstrated that the HRBF experiment achieved the lowest average MAE of 1.12 bpm, whereas the HRWB experiment recorded the highest average MAE of 4.2 bpm.

Therefore, the proposed technique is crucial for accurately extracting neonatal cardiac signals under UV illumination, compared to the results obtained without using the blue filter method in the HRWB experiment.

This methodology is considered novel and more effective in the neonatal healthcare system, particularly in the rise in contagious viral infections such as COVID-19.

5 Discussion

This study focuses on the urgent need for a neonatal healthcare noncontact system to monitor HR values under UV illumination during the spread of transitional epidemics like COVID-19 and other new diseases. The main goal of the research was to develop a neonatal healthcare noncontact system that combines noncontact technology and image processing to accurately evaluate the heart rate of neonates using noncontact camera technology during an emergency. The proposed blue filter technique, combined with the EVM method, was utilized to extract cardio signals effectively to enhance the accuracy and reliability of signal detection by reducing the interference caused by UV illumination and amplifying the subtle temporal color variations in the skin. The blue filter was specifically employed to balance the intensity of the color channels under UV light, mitigating the impact of excess blue or red light reflections and isolating the green channel, which is most sensitive to pulsatile blood flow.

The proposed approach was critical for ensuring precise cardiac signal extraction in neonates exposed to UV illumination compared with obtained results without using a blue filter method in the HRWB experiment.

Also, this approach for skin color magnification offers several advantages. Enhancing skin color variations in the temporal domain enhances signal clarity without requiring physical contact, making it ideal for neonatal applications. Furthermore, the reduction in computational overhead ensures that the method is deployable in real-time monitoring systems, an essential criterion for practical implementation in NICU settings.

The effectiveness of this technique was demonstrated through a comparative analysis of video sequences with and without magnification. This advancement not only accelerates execution time but also increases the robustness of non-contact physiological monitoring solutions.

On the other hand, this study highlights the effectiveness of the ROI tile-based selection method in monitoring vital signs, demonstrating improved adaptability to neonatal movements and potentially reducing the need for manual adjustments. The primary challenges encountered in this study are outlined as follows:

1. The difficulty of acquiring a sufficiently large dataset of infants under UV illumination, compounded by their critical health conditions.
2. The presence of complex medical apparatus obstructs the capture of the neonate's body posture, thereby limiting the effectiveness of the monitoring system.
3. The presence of NICU personnel, such as nurses and doctors, or items like toys that resemble infants, particularly when they are situated on bedsheets, can lead to false detection incidents.
4. The data acquisition process was time-consuming and required effort, especially given the requirement for each neonate to be recorded multiple times in their most appropriate posture. UV illumination and lighting variability.
5. One of the significant challenges was ensuring accurate performance validation by recording neonatal data under both UV and non-UV illumination as the same subjects. This challenge necessitated additional work to mitigate disparities across channels in the equalized phototherapy image to simulate natural lighting conditions.

Table 1 Comparison the proposed system (HRBF) with the previous studies.

Authors	Sensor	ROI	Technique	Region	MAE (bpm)	PCC, SCC
Poh et al. [34]	Video camera	Bounding box	Chrominance	Face	3	0.98,−
Wei et al. [35]	Video camera	Bounding box	ICA	Face	2.65	0.92,−
Wang et al. [36]	RBG camera	Tile	Spatial processing	Wrist	−,−	−,−
Revanur et al. [37]	Video Footage	−	Video Transformer	Face	13	−,−
Molinaro et al. [38]	Digiatl camer	−	PPG	Face	5	−,−
Cheng et al. [39]	RGB Camera	Bounding box	EEMD	Face	−	0.96, −
Sharma et al. [32]	Low-cost video camera	Bounding box	FFT	Face	−	−,−
Stockwell et al. [40]	Forehead-based PPG sensor	Bounding box	Reflection mode PPG	Forehea d	8.44	−,0.981
Al-Naji et al. [41]	Digital camera	Bounding box	Noise artifact removal	Face	2.91	0.97, −
Khanam et al. [42]	Digital camera	IImage decomposition	Color based method	Face	3.56	0.979,−
Alnaggar et al. [31]	RGB Camera	Tile	EVM	chest	1.62	−,−
HRBF (Our proposed)	Nikon D3500	Tile	Blue filer, EVM	Face	1.12	0.998, 0.982

To evaluate the efficacy of our findings from the HRBF experiment. We compared them with 11 reliable studies using non-contact technology-based monitoring methods, as shown in Table 1. The findings indicated that the suggested system achieved the lowest average MAE of 1.12 bpm and exhibited high PCC and SCC metrics of 0.997 and 0.982, respectively. The error rate study indicates that the proposed blue filter technique combined with the proposed tile- based ROI selection method significantly enhances the accuracy of HR values in comparison to previous studies. The suggested technique is appropriate for use in healthcare or indoor home monitoring.

6 Conclusions

In conclusion, this study introduced a novel non-contact neonatal heart rate monitoring for neonates under UV illumination, addressing the limitations of traditional contact-based monitoring devices. A robust tile-based ROI selection method for neonatal cardiac signal monitoring was introduced, ensuring accurate heart rate calculation despite infant movements and eliminating the need for manual bounding box adjustments. A blue filter technique combined with the EVM method was utilized to enhance the extraction of cardiac signals by mitigating interference from UV illumination and amplifying subtle temporal skin color variations. Furthermore, a specialized neonatal GUI was developed, offering a user-friendly platform for biomedical engineers to monitor vital signs remotely in the neonatal NICU. Experimental results demonstrated the system's efficacy, achieving high correlation coefficients (PCC = 0.998) and low error rates (MAE = 1.12 bpm) in the HRBF experiment, outperforming results from the HRWF experiment (PCC = 0.981; MAE = 4.2 bpm). The system's low cost and ease of deployment position it as a viable solution for real-time neonatal healthcare monitoring system, particularly during transitional epidemics like COVID-19 and other scenarios requiring reduced physical contact. Future work will focus on enhancing system reliability by integrating advanced signal processing techniques and exploring machine learning approaches to optimize ROI selection and improve overall performance.

Acknowledgments

The author would like to thank the staff of the Department of Medical Instrumentation Techniques Engineering, Electrical Engineering Technical College, Middle Technical University, for their support during this work.

Disclosures

The authors have no competing interests to declare that are relevant to the content of this article.

References

1. D. McDuff, S. Gontarek, and R. W. Picard, "Improvements in remote cardiopulmonary measurement using a five band digital camera," IEEE Transactions on Biomedical Engineering 61(10), 2593–2601 (2014).
2. A. G. Shabeeb, H. A. Hashim, and S. K. Gharghan, "Heart disease classification based on combination of PCA /ANFIS model," Research on Biomedical Engineering 40(3), 609–625 (2024).
3. X. He, R. A. Goubran, and X. P. Liu, "Wrist pulse measurement and analysis using Eulerian video magnification," IEEE-EMBS International Conference on Biomedical and Health Informatics (BHI), 41–44 (2016).
4. N. Kumar, G. Akangire, B. Sullivan, K. Fairchild, and V. Sampath, "Continuous vital sign analysis for predicting and preventing neonatal diseases in the twenty-first century: big data to the forefront," Pediatric Research 87(2), 210–220 (2020).
5. H. Ali Hashim, N. Mahmood Ahmed, and A. G. Shabeeb, "Infant heart rate estimation based on non-contact UV photoplethysmography," Indonesian Journal of Electrical Engineering and Computer Science 31(1), 180 (2023).
6. D. Kolosov, V. Kelefouras, P. Kourtessis, and I. Mporas, "Contactless camera-based heart rate and respiratory rate monitoring using ai on hardware," Sensors 23(9), 4550 (2023).
7. L. Scalise, N. Bernacchia, I. Ercoli, and P. Marchionni, "Heart rate measurement in neonatal patients using a webcamera," IEEE International Symposium on Medical Measurements and Applications Proceedings, IEEE, Budapest, Hungary (2012).
8. J. Brieva, E. Moya-Albor, O. Rivas-Scott, and H. Ponce, "Non-contact breathing rate monitoring system based on a Hermite video magnification technique," in 14th International Symposium on Medical Information Processing and Analysis, SPIE Proceedings 10975, 1097504 (2018).
9. M. Chen, Q. Zhu, H. Zhang, M. Wu, and Q. Wang, "Respiratory rate estimation from face videos," 2019 IEEE EMBS International Conference on Biomedical & Health Informatics, Chicago, IL, USA (2019).
10. H. A. Hashim, "Non-contact automatic respiratory rate monitoring for newborns using digital camera technology and deep learning," Journal of Biomedical Photonics & Engineering 10(4), 040317 (2024).
11. A. Al-Naji, K. Gibson, S.-H. Lee, and J. Chahl, "Monitoring of cardiorespiratory signal: principles of remote measurements and review of methods," IEEE Access 5, 15776–15790 (2017).
12. A. Al-Naji, A. G. Perera, and J. Chahl, "Remote monitoring of cardiorespiratory signals from a hovering unmanned aerial vehicle," Biomedical Engineering Online 16(1), 101 (2017).

13. W. Verkruysse, L. O. Svaasand, and J. S. Nelson, "Remote plethysmographic imaging using ambient light," Optics Express 16(26), 21434 (2008).
14. L. Tarassenko, M. Villarroel, A. Guazzi, J. Jorge, D. A. Clifton, and C. Pugh, "Non-contact video-based vital sign monitoring using ambient light and auto-regressive models," Physiological Measurement 35(5), 807–831 (2014).
15. Y. Zeng, D. Yu, X. Song, Q. Wang, L. Pan, H. Lu, and W. Wang, "Camera-based cardiorespiratory monitoring of preterm infants in NICU," IEEE Transactions on Instrumentation and Measurement 73, 1–13 (2024).
16. G. O. Ganfure, "Using video stream for continuous monitoring of breathing rate for general setting," Signal, Image and Video Processing 13(7), 1395–1403 (2019).
17. H. Qi, Z. Guo, X. Chen, Z. Shen, and Z. Jane Wang, "Video-based human heart rate measurement using joint blind source separation," Biomedical Signal Processing and Control 31, 309–320 (2017).
18. H. Hashim, S. Mohammed, and S. Gharghan, "Accurate localization of elderly people based on neural and wireless sensor networks," Journal of Engineering and Applied Science 14(11), 3777–3789 (2019).
19. C. Gonzalez Viejo, S. Fuentes, D. D. Torrico, and F. R. Dunshea, "Non-contact heart rate and blood pressure estimations from video analysis and machine learning modelling applied to food sensory responses: a case study for chocolate," Sensors 18(6), 1802 (2018).
20. Y. Sun, C. Papin, V. Azorin-Peris, R. Kalawsky, S. Greenwald, and S. Hu, "Use of ambient light in remote photoplethysmographic systems: comparison between a high-performance camera and a low-cost webcam," Journal of Biomedical Optics 17(3), 037005 (2012)
21. A. Al-Naji, J. Chahl, "Remote respiratory monitoring system based on developing motion magnification technique," Biomedical Signal Processing and Control 29, 1–10 (2016).
22. K. S. Tan, R. Saatchi, H. Elphick, and D. Burke, "Real-time vision based respiration monitoring system," in 7th International Symposium on Communication Systems, Networks & Digital Signal Processing, 770–774 (2010).
23. M. Bartula, T. Tigges, and J. Muehlsteff, "Camera-based system for contactless monitoring of respiration," 35th Annual International Conference of the IEEE Engineering in Medicine and Biology Society 2672–2675 (2013).
24. K.-Y. Lin, D.-Y. Chen, and W.-J. Tsai, "Face-based heart rate signal decomposition and evaluation using multiple linear regression," IEEE Sensors Journal 16(5), 1351–1360 (2016).
25. D.-Y. Chen, J.-J. Wang, K.-Y. Lin, H.-H. Chang, H.-K. Wu, Y.-S. Chen, and S.-Y. Lee, "Image sensor-based heart rate evaluation from face reflectance using hilbert–huang transform," IEEE Sensors Journal 15(1), 618–627 (2015).
26. W. Wang, S. Stuijk, and G. de Haan, "A novel algorithm for remote photoplethysmography: Spatial subspace rotation," IEEE Transactions on Biomedical Engineering 63(9), 1974–1984 (2016).
27. S. Yu, S. Hu, V. Azorin-Peris, J. A. Chambers, Y. Zhu, and S. E. Greenwald, "Motion-compensated noncontact imaging photoplethysmography to monitor cardiorespiratory status during exercise," Journal of Biomedical Optics 16(7), 077010 (2011).
28. L. A. M. Aarts, V. Jeanne, J. P. Cleary, C. Lieber, J. S. Nelson, S. Bambang Oetomo, and W. Verkruysse, "Non-contact heart rate monitoring utilizing camera photoplethysmography in the neonatal intensive care unit — A pilot study," Early Human Development 89(12), 943–948 (2013).
29. K. Gibson, A. Al-Naji, J. Fleet, M. Steen, A. Esterman, J. Chahl, J. Huynh, and S. Morris, "Non-contact heart and respiratory rate monitoring of preterm infants based on a computer vision system: a method comparison study," Pediatr Research 86(6), 738–741 (2019).
30. M.-Z. Poh, D. J. McDuff, and R. W. Picard, "Advancements in noncontact, multiparameter physiological measurements using a webcam," IEEE Transactions on Biomedical Engineering 58(1), 7–11 (2011).
31. M. Alnaggar, A. I. Siam, M. Handosa, T. Medhat, and M. Z. Rashad, "Video-based real-time monitoring for heart rate and respiration rate," Expert Systems with Applications 225, 120135 (2023).
32. N. Sharma, S. Kaman, and P. K. Mahapatra, "Non-contact measurement of human heart rate using low cost video camera," 2019 Fifth International Conference on Image Information Processing, 58–62 (2019).
33. Z. Wu, N. E. Huang, "Ensemble empirical mode decomposition: a noise-assisted data analysis method," Advances in Adaptive Data Analysis 01(01), 1–41 (2009).
34. M.-Z. Poh, D. J. McDuff, and R. W. Picard, "Non-contact, automated cardiac pulse measurements using video imaging and blind source separation," Optics Express 18(10), 10762 (2010).
35. W. Wei, K. Vatanparvar, L. Zhu, J. Kuang, and A. Gao, "Remote photoplethysmography and heart rate estimation by dynamic region of interest tracking," in 44th Annual International Conference of the IEEE Engineering in Medicine & Biology Society, 3243–3248 (2022).
36. H. Wang, S. Zhang, "Non-contact heart rate measurement using low-cost RGB camera under complex light conditions," Multimedia Tools and Applications 84(3), 1561–1575 (2025).
37. A. Revanur, A. Dasari, C. S. Tucker, and L. A. Jeni, "Instantaneous physiological estimation using video transformers," in Multimodal AI in Healthcare, A. Shaban-Nejad, M. Michalowski, and S. Bianco (Eds.), Springer International Publishing 1060, 307–319 (2023).
38. N. Molinaro, F. Zangarelli, E. Schena, S. Silvestri, and C. Massaroni, "Cardiorespiratory parameters monitoring through a single digital camera in real scenarios: ROI tracking and motion influence," IEEE Sensors Journal 23(17), 20097–20106 (2023).

39. J. Cheng, X. Chen, L. Xu, and Z. J. Wang, "Illumination variation-resistant video-based heart rate measurement using joint blind source separation and ensemble empirical mode decomposition," IEEE Journal of Biomedical and Health Informatics 21(5), 1422–1433 (2017).
40. S. J. Stockwell, T. C. Kwok, S. P. Morgan, D. Sharkey, and B. R. Hayes-Gill, "Forehead monitoring of heart rate in neonatal intensive care," Frontiers in Physiology 14, 1127419 (2023).
41. A. Al-Naji, J. Chahl, "Remote optical cardiopulmonary signal extraction with noise artifact removal, multiple subject detection & long-distance," IEEE Access 6, 11573–11595 (2018).
42. F.-T.-Z. Khanam, A. Al-Naji, A. G. Perera, K. Gibson, and J. Chahl, "Remote vital signs monitoring in neonatal intensive care unit using a digital camera," International Journal of Biomedical and Biological Engineering 16(10), 138–144 (2022).